

Chapter 4

Realization of MQ Experiment

In this section some practical hints will be elucidated for realization of MQ experiment. It will be shown that TPPI in two-dimensional experiment (see sections 2.4.3 and 2.5.2) can be sometimes replaced by hypercomplex ([Ern87, SR94]) method for recoding the data. Also experimental methods like DQ filtering and phase cycling for removing spectrometer errors will be presented, respectively.

4.1 Spectrometer

To perform MQ experiment fast electronic which allows quick switching between r.f. pulses has to be available. To achieve high resolution of MQ spectra also high B_0 fields are preferred. In this work Varian Unity Plus and later Unity INOVA has been used to perform experiments with $B_0 = 9.4$ T corresponding to 400 MHz for protons 1H . Short switching delays are especially important for C7, POST C7 as well as for BABA pulse sequences. In our case the minimal time between r.f. pulses until the phase is settled has been $0.2 \mu s$ for phases differing in 90° . In addition NMR spectrometer has to be equipped to perform r.f. pulses with phases which differ in phase smaller than 90° called *small angle phase switching*. Also strong B_1 r.f. fields allowing short r.f. pulses (of order of $3 \mu s$) for proton experiments are an advantage especially for pulse sequences working with δ -like pulses (DRAMA, BABA, eight and thirty-two pulse sequences).

4.1.1 Requirements for MAS

To realize MAS experiment, probes which allows high spinning speeds are required. Measured sample has to be filled into the cylindrical rotor closed by the cap which rotate

about the axes tilted from the \vec{B}_0 field by *magic angle* 54.7° . Nowadays the rotors are made by ceramic materials like Zirconia-oxid (ZrO_2) or Silicon Nitride (Si_3N_4), which have proper mechanical features under high spinning speeds in the presence of magnetic field. They should not be made from materials, which consists of the same nuclei as an investigated sample to prevent overlapping of the signals. Due to the high rotational frequencies ($f_r \geq 10$ kHz) the centrifugal force acting on the outer wall of the rotor is very high which has to be also taken into account for the design of the rotor. The high spinning caps (schematically shown in Figure 1.3a) usually made from Torlon has a special design to allow high rotations realized by driven-air. To get the stable rotation the rotor is surrounded by the bearing-air flow which can be regulated independently to the driven-air. The resulting rotational frequency f_r can be regulated by the increasing or decreasing of the driving-air pressure. For all MAS experiments in this work rotors with an average of the cylinder of 5 mm are used. They allow to rotate up to $f_r = 13$ kHz. To get better B_1 field homogeneity the sample should not exceed the size of the r.f. coil which can be achieved by the filling of the rotor by the Teflon cylindrical fillers inserted from both sides of the sample.

4.2 Hypercomplex versus TPPI acquisition

In two-dimensional (2D) DQ spectroscopy it is sometimes preferred to record the DQ signal in the sense of *hypercomplex* data sets ([Ern87, SR94]) instead of TPPI (see e.g. section 2.4.3) data sets. When it is useful will be discussed in this section.

Intensity of the DQ signal can be written according to equations (3.14), (3.17) and (3.26) in general in the form

$$S_I^{DQ}(t_1, t_2 = 0) = \cos\left(2 \Delta\omega_\phi t_1 + \Omega(t_1)\right) I_{DQ}, \quad (4.1)$$

where I_{DQ} represents the amplitude of DQ signal. The *cos* term in equation (4.1) determines the phase of the DQ signal. For pulse sequences acting under MAS like DRAMA, BABA, C7 or POST C7 factor $\Omega(t_1)$ represents rotor modulation of the DQ signal. It can be $\Omega(t_1) = \omega_r t_1$ for C7/POST C7 pulse sequence or $\Omega(t_1) = k \cdot \omega_r t_1$ ($k = \pm 1, \pm 3, \pm 5, \dots$)¹ for DRAMA/BABA pulse sequence. For eight pulse sequence and thirty-two pulse sequence $\Omega(t_1) = 0$, so there is no rotor modulation (see equation (3.26)).

¹More details about DQ signal for DRAMA/BABA pulse sequence see equation (3.14).

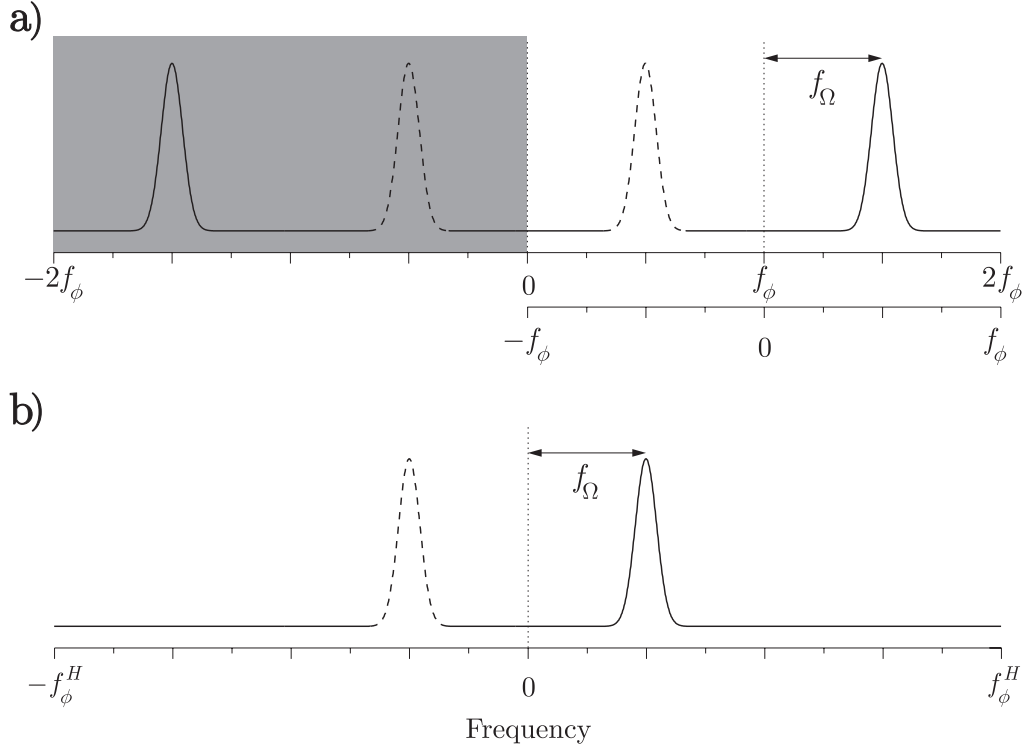


Figure 4.1: Comparison of TPPI a) and hypercomplex b) sampling of the data in DQ spectroscopy. Shaded area in figure a) corresponds to the mirroring of the right part of the spectrum due to the cosine Fourier transformation. Frequency f_Ω describes the rotor modulation of the DQ signal. It is $f_\Omega = f_r$ for C7/POST C7 pulse sequence and $f_\Omega = k \cdot f_r$ for DRAMA/BABA pulse sequence, respectively. Dashed peaks represent symbolically negative first-order spinning sideband ($k = -1$) for DRAMA/BABA pulse sequence (see section 3.2.1).

If we choose in TPPI experiment $2\Delta\omega_\phi t_1 = \frac{\pi}{2}m$ in equation (4.1), where $m = 0, 1, 2, \dots$ represents time proportional incrementing of the phase of the r.f. pulses during excitation period ($t_1 = \Delta t_1 \cdot m$) the DQ signal will follow the scheme

$$\cos(\Omega(0))I_{DQ}, \sin(\Omega(\Delta t_1))I_{DQ}, -\cos(\Omega(2\Delta t_1))I_{DQ}, -\sin(\Omega(3\Delta t_1))I_{DQ}, \dots \quad (4.2)$$

This directly corresponds to the sampling of the data in the sense of Redfield ([Red75]). Hence, this acquisition technique allows to distinguish between positive and negative frequencies even when no imaginary part of the signal in ω_1 dimension is available. Cosine Fourier transformation of the DQ signal recorded in the sense of scheme (4.2) leads to the spectrum shown in Figure 4.1a. Only the right part of the full spectrum in Figure 4.1a represent the correct spectrum. To display it in the proper way the scale has to be changed as it is indicated. Thus, in TPPI experiment recorded by this technique only frequencies

inside of the 'Nyquist zone' ([SR94]) between positive and negative Nyquist frequencies $\pm f_\phi = \pm(4\Delta t_1)^{-1}$ can be seen. To prevent aliasing of the signal from outside of the Nyquist zone, f_ϕ has to be chosen in 2D DQ experiment as

$$f_\phi \geq f_r \quad \text{and} \quad f_\phi \geq |k| \cdot f_r \quad (k = \pm 1, \pm 3, \dots) \quad (4.3)$$

for C7/POST C7 and for DRAMA/BABA² pulse sequences, respectively.

Instead of TPPI it follows from equation (4.1) that DQ signal can be recorded in the sense of *hypercomplex* data sampling if $2\Delta\omega_\phi t_1 = \frac{\pi}{2}m$ and $m = 0, 1$ without incrementing the time t_1 . Hence DQ signal will follow the scheme³

$$\begin{aligned} &\cos(\Omega(0)) I_{DQ}, \cos(\Omega(\Delta t_1)) I_{DQ}, \dots \\ &\sin(\Omega(0)) I_{DQ}, \sin(\Omega(\Delta t_1)) I_{DQ}, \dots \end{aligned} \quad (4.4)$$

Fourier transformation of this signal leads directly to the spectrum shown in Figure 4.1b where positive and negative frequencies are clearly distinguished. Nyquist zone is in this case defined by the Nyquist frequency $\pm f_\phi^H = \pm(2\Delta t_1)^{-1}$.

Comparing TPPI and *hypercomplex* acquisition with connection to the DQ spectroscopy one might think that hypercomplex method of sampling of the data is preferred due to its twice higher Nyquist frequency $f_\phi^H = 2f_\phi$. In fact the cost of this is recording twice number of data points in ω_1 dimension, thus, measuring time is doubled. It has to be noted that the same conditions can be achieved by TPPI choosing the sampling period half of the original one presented by acquisition scheme (4.2), $\Delta t_1 \rightarrow \Delta t_1/2$, and increasing twice number of measuring points. Hence, TPPI and hypercomplex acquisition in DQ spectroscopy will become equivalent.

In fact *hypercomplex* acquisition may be preferred for C7 as well as for POST C7 pulse sequences in DQ spectroscopy. Cumbersome mirroring (see shaded area in Figure 4.1a) caused by recording the data in the sense of Redfield ([Red75]) is overcome by hypercomplex data sampling. In addition if for some reasons (caused by e.g. r.f. pulse imperfections) double quantum filtration (see section 4.3) will not work properly, the remaining part of the initial Zeeman order described by the first term in equation (3.17) (see section 3.2.2) appear in the spectrum. It is important to note that it will appear in the middle of the spectrum in Figure 4.1b, thus, it will not disturb DQ signal if rotational frequency f_r is

² k represents the highest DQ spinning sideband order in the ω_1 dimension (see section 3.2.1).

³Second two data sets rising from ω_2 dimension are for simplicity omitted (more details see e.g. [SR94]).

high enough. On the other hand hypercomplex acquisition is not preferred for DRAMA as well as for BABA pulse sequences. The first term in equation (3.11) despite of C7 pulse sequence is rotor modulated and in the case of hypercomplex acquisition will merge with DQ signal. Hence, TPPI method where this problem is overcome by shifting of the DQ signal to the frequency $f_\phi + k \cdot f_r$ ($k = \pm 1, \pm 3, \dots$) is preferred for DRAMA and BABA pulse sequences. To prevent overlapping of DQ signal in TPPI method with mentioned remaining part of the initial Zeeman order enough small sampling interval Δt_1 has to be chosen to fit all expected DQ sidebands to the spectrum without overlapping and aliasing.

4.3 Double quantum filtering

Multiple quantum (MQ) filtration techniques are often used to select desired order of coherence and suppress other coherent transitions. Characteristic response to a phase shift ϕ of the r.f. pulses used during excitation period to a p -quantum coherence can be written as ([Mun87, Wei83])

$$\hat{\rho}^p(\phi) = \hat{\rho}^p(0) e^{-ip\phi}, \quad (4.5)$$

where $\hat{\rho}^p(\phi)$ describes coherence order p according to the phase ϕ . This behaviour can be used to select coherences of order p .

If phase between excitation and reconversion period (see e.g. Figure 2.12) is incremented in steps of $\Delta\phi = \frac{\pi}{p}$ after each experiment and, in addition, experiments are step by step added and subtracted, all coherences p' up to the certain order⁴ which differ from p , $|p'| \neq |p|$, will be filtered out from the spectrum. To realize this selection of p -quantum coherence one need $2p$ sets of data. To proof this p -quantum filter the intensity of p' -quantum coherence $I_{MQ,p'}$ can be calculated as ([Bod81, Gra97a])

$$I_{MQ,p'} = \sum_{k=0}^{2p-1} (-1)^k e^{-i\frac{\pi}{p}p'k} = \sum_{k=0}^{2p-1} e^{-i\frac{\pi}{p}(p-p')k}. \quad (4.6)$$

In the last summation the relation $(-1)^k = e^{i\pi k}$ is used. It can be directly seen from equation (4.6) that for $p' = \pm p$ the exponent is 0 or 2π , thus, the full intensity of coherence order p equal to $2p$ will be seen. To calculate intensities of orders $|p'| \neq |p|$ summation in equation (4.6) can be expressed as a geometrical series as

$$I_{MQ,p'} = \frac{e^{i2\pi(p-p')} - 1}{e^{i\frac{\pi}{p}(p-p')} - 1}. \quad (4.7)$$

⁴See later discussion.

ϕ_{exc}	ϕ_{ref}
0°	0°
90°	180°
180°	0°
270°	180°

Table 4.1: Phase cycling to select DQ coherence ($p = 2$).

Analysing equation (4.7) it can be seen that nearly all coherences $p' \in \mathbf{N}$ are filtered out. Only coherences where also denominator is zero i.e. $p' = p(2k + 1)$, where $k \in \mathbf{N}$ can not be filtered out from the spectrum by this p -quantum filter.

To realize double quantum (DQ) filter ($p = 2$), it follows from above discussion, it is sufficient to add and subtract four different coherences. The phase of the r.f. pulses acting during excitation period is then advanced in increments of $\frac{\pi}{2}$ (90°) which cause the DQ signal to alternate in sign. The phases of excitation period ϕ_{exc} and reference frequency (receiver phase) ϕ_{ref} are shown for DQ filter in Table 4.1. It has to be noted that coherences of order 6, 10, 14, \dots will be not filtered out from the spectrum. Hence, this filter is $4k + 2$ ($k \in \mathbf{N}$) quantum selective. To realize even higher selectivity more sophisticated approach proposed by Wokaun and Ernst ([Wok77]) can be used. Disadvantage of this method is that it requires $2p_{max}$ different two-dimensional experiments which are stored separately, where p_{max} is the maximum desired order of coherence to be filtered out. Hence, to distinguish 6-quantum coherence from DQ coherence it would be necessary to record separately 12 two-dimensional experiments. This would increase measuring time three times with comparison to the DQ filter presented in Table 4.1. Nevertheless, if higher order coherences are expected to see in the MQ experiment this price has to be payed for selecting DQ coherence, if good results are required.

4.4 MQ phase cycling techniques

In MQ spectroscopy only rarely multiple-pulse sequences generate pure MQ coherences according to the theoretical predictions. It is often necessary to use sophisticated phase cycling techniques to remove spurious signals coming from r.f. pulse imperfections as well as from background signals. In this work mainly two different phase cycling techniques were

ϕ_{exc}	ϕ_{rec}	ϕ_{det}	ϕ_{ref}	$\phi_{rec}^{32+...}$	$\phi_{det}^{32+...}$	$\phi_{ref}^{32+...}$
$0^\circ + \phi$	90°	0°	0°	0°	0°	180°
$90^\circ + \phi$	90°	0°	180°	0°	0°	0°
$180^\circ + \phi$	90°	0°	0°	0°	0°	180°
$270^\circ + \phi$	90°	0°	180°	0°	0°	0°
$0^\circ + \phi$	90°	180°	180°	0°	180°	0°
$90^\circ + \phi$	90°	180°	0°	0°	180°	180°
$180^\circ + \phi$	90°	180°	180°	0°	180°	0°
$270^\circ + \phi$	90°	180°	0°	0°	180°	180°
$0^\circ + \phi$	90°	90°	90°	0°	90°	270°
$90^\circ + \phi$	90°	90°	270°	0°	90°	90°
$180^\circ + \phi$	90°	90°	90°	0°	90°	270°
$270^\circ + \phi$	90°	90°	270°	0°	90°	90°
$0^\circ + \phi$	90°	270°	270°	0°	270°	90°
$90^\circ + \phi$	90°	270°	90°	0°	270°	270°
$180^\circ + \phi$	90°	270°	270°	0°	270°	90°
$270^\circ + \phi$	90°	270°	90°	0°	270°	270°
$0^\circ + \phi$	270°	0°	0°	180°	0°	180°
$90^\circ + \phi$	270°	0°	180°	180°	0°	0°
\vdots	\vdots	\vdots	\vdots	\vdots	\vdots	\vdots

Table 4.2: Phase cycling for DQ filtered experiment. It can be performed in steps of 4, 8, 16, 32 or 64 increments. Phase ϕ corresponds to the TPPI or hypercomplex acquisition (see section 4.2). In TPPI DQ experiment it is varied in steps of $\Delta\phi = 45^\circ$ as $\phi = \{0, 45^\circ, 90^\circ, 135^\circ, 180^\circ, 225^\circ, 270^\circ, 315^\circ\}$ with respect to evolution time t_1 .

used. The first one in the connection to the DQ spectroscopy presented in sections 3.3 and 3.5.1 where DQ filtering (see section 4.3) was used to select DQ coherence. This phase cycling of excitation ϕ_{exc} and reconversion ϕ_{rec} period, detecting pulse ϕ_{det} , and reference frequency (receiver phase) ϕ_{ref} is shown in Table 4.2, respectively. It was adopted from Gottwald ([Got96]) and extended to the full compensation 64 phase cycle to remove even more artifacts. The second phase cycling technique has been used in spin counting experiments in section 3.4 for MAS experiments as well as in section 3.5.2 for experiments

ϕ_{exc}	ϕ_{rec}	$\phi_{det} = \phi_{ref}$
$0^\circ + \phi$	90°	0°
$0^\circ + \phi$	90°	90°
$0^\circ + \phi$	90°	180°
$0^\circ + \phi$	90°	270°
$180^\circ + \phi$	270°	0°
$180^\circ + \phi$	270°	90°
$180^\circ + \phi$	270°	180°
$180^\circ + \phi$	270°	270°
$90^\circ + \phi$	180°	0°
$90^\circ + \phi$	180°	90°
$90^\circ + \phi$	180°	180°
$90^\circ + \phi$	180°	270°
$270^\circ + \phi$	0°	0°
$270^\circ + \phi$	0°	90°
$270^\circ + \phi$	0°	180°
$270^\circ + \phi$	0°	270°

Table 4.3: Phase cycling for spin counting MQ experiment. Phase of a detecting pulse ϕ_{det} and a reference (receiver) phase ϕ_{ref} has to be cycled synchronically. Phases 0° , 90° , 180° and 270° correspond to the phases of r.f. pulses marked in this work as x , y , \bar{x} , and \bar{y} , respectively.

without MAS. The phase cycle is shown in Table 4.3. It is in principle modified CYCLOPS (cyclically ordered pulse sequence, [Ste74a, Ste74b]) for MQ excitation. To perform full compensation 16-step phase cycle is sufficient to remove all possible artifacts coming from r.f. pulse imperfections. The phase of the reconversion period can not be set arbitrary. It has to follow excitation period to achieve proper time reversal (see section 2.3.1).